Research Square

Preprints are preliminary reports that have not undergone peer review.
They should not be considered conclusive, used to inform clinical practice,
or referenced by the media as validated information.

Functional Insights into Leishmania braziliensis PDI2: Implications for Pharmacological Susceptibility

PEM Villanueva
Universidad Nacional de Colombia-Sede Bogotá
Esteban León
Universidad Nacional de Colombia-Sede Bogotá
Adrián G Sandoval-Hernández
Universidad Nacional de Colombia
María H Ramírez-Hernández
Universidad Nacional de Colombia-Sede Bogotá
Luis E. Contreras R
lecontrerasr@unal.edu.co
Universidad Nacional de Colombia-Sede Bogotá

Research Article

Keywords: CRISPR/Cas9, Knockout, EC50, Leishmania braziliensis, Protein Disulfide Isomerase 2, Ketoconazole, Geneticin G418, Trivalent antimony (Sb3+)

Posted Date: September 30th, 2026

DOI: https://doi.org/10.21203/rs.3.rs-10944722/v1

License: This work is licensed under a Creative Commons Attribution 4.0 International License.
Read Full License

Additional Declarations: No competing interests reported.

Abstract

Leishmaniasis is a highly prevalent parasitic neglected disease caused by protozoa of the genus *Leishmania*. Currently, there are no vaccines available for human use, and existing treatments are ineffective due to toxicity and the emergence of drug-resistant strains. Then, it is necessary the identification of new molecular targets. In this study, a candidate protein disulfide isomerase 2 in *L. braziliensis* (LbPDI2) was identified and analyzed, with particular emphasis on its role in pharmacological susceptibility. A bioinformatic search based on conserved PDI2 sequences identified a single high-confidence candidate in the M2903 reference genome (LBRM2903_350086300.1) displaying canonical features, including two CGHC catalytic motifs, four functional domains (A, B, B', A'), a signal peptide, and an ER retention sequence (EGDL). Structural modelling revealed a reliable and flexible U-shaped fold, which is typical of PDIs. A CRISPR/Cas9-mediated replacement of *Lbpdi2* gene was verified by UTR-spanning PCR and junction sequencing. The resulting *Lbpdi2*$^{-/-}$ promastigotes showed no significant differences in growth compared to wild-type parasites, indicating that the LbPDI2 candidate is not essential for basal proliferation. However, drug susceptibility assays exhibited that *Lbpdi2* deletion alters the parasite's response to pharmacological stress. Mutant parasites exhibited increased resistance to Sb^{3+} and heightened sensitivity to the ribosome inhibitor G418 and the sterol biosynthesis inhibitor ketoconazole. In contrast, no significant changes were observed with hydrogen peroxide. These findings identify the LbPDI2 candidate as a conserved, likely ER-localized protein linked to altered *in vitro* drug responses in *L. braziliensis* promastigotes, highlighting its potential as a therapeutic target.

1. INTRODUCTION

Leishmaniasis is a parasitic disease classified as a neglected tropical disease (NTD), caused by flagellated protozoa of the genus *Leishmania*. Twenty species capable of infecting humans have been identified, nine of which are present in Colombia, affecting populations with limited access to basic healthcare services. The influence of species diversity on clinical manifestations, disease severity, diagnostic accuracy and treatment response is well-documented. The fact that this disease is endemic in over 102 countries, with a high rate of morbidity and mortality, makes it a significant public health concern. Globally, the prevalence of the infection is estimated at around 12 million infected people (including asymptomatic cases), 350 million people at risk of infection, and between 0.6 and 1.0 million new cases each year (Mann et al. 2021).

There are currently no vaccines available for human leishmaniasis, and patient management relies on drugs that are unsatisfactory due to several factors, including cost, toxicity, route of administration and the existence of drug-resistant strains (Alpizar-Sosa et al. 2022). Nevertheless, treatment of the disease continues using antimony salts, such as Glucantime and Pentostam, which are recognised as first-line drugs. Amphotericin B, pentamidine isetionate, miltefosine, ketoconazole and paromomycin, constitute second-line drugs (Dinc 2022).

The efficacy of antimony is gradually declining, resulting in treatment failure rates of around 65% (Gutierrez Guarnizo et al. 2023). In the context of antimony-resistant strains of *L. tropica* and *L. panamensis*, an elevated expression of diverse proteins has been documented, including protein disulfide isomerase 2 (PDI2) (Peláez et al. 2012; Tasbihi et al. 2020).

PDIs are encoded by conserved genes in *Leishmania* and are structurally and functionally similar to PDIs in higher eukaryotes, exhibiting reductase, isomerase and/or chaperone activity (Dousti et al. 2023). PDI2 is composed of four thioredoxin (Trx) domains (A, B, B' and A'), a linker region and an alpha-helical domain at the C-terminal end, which contains the sequence required for its retention in the endoplasmic reticulum (ER). Domains A and A' contain the active redox site Cys-X-X-Cys (CXXC), which catalyzes thiol-disulfide exchange reactions during substrate folding, while domains B and B' provide the primary substrate-binding site by forming a hydrophobic interaction pocket (Matsusaki et al. 2020).

Although transcriptomic and proteomic profiles have documented the expression of LbPDI2 and suggested its role as a key virulence factor in *L. braziliensis* (Cuervo et al. 2009), these findings depend on sequence-based bioinformatic annotations. Consequently, despite its mention in previous omics studies, a detailed study of its physicochemical and structural characteristics, as well as its role in the parasite's response to pharmacological treatments, has not yet been reported.

In this study, bioinformatic and experimental approaches were employed to identify and analyze candidate genes encoding PDIs in *L. braziliensis*, with a particular focus on LbPDI2. This approach generated predictive structural insights and a PDI2-deficient mutant parasite line, for which susceptibility to different pharmacological agents was assessed.

2. MATERIAL AND METHODS

1. Bioinformatics approach

1.1 Identification and *in silico* characterization of a candidate for LbPDI2.

Multiple alignment of three experimentally characterized primary structures of PDI2 belonging to different *Leishmania* species was performed in Jalview 2.11.5.1 using the T-Coffee option with the default parameters (Notredame et al. 2000; Waterhouse et al. 2009). The sequences of *L. amazonensis* (TriTrypDB ID: LAMA_000377400), *L. major* (TriTrypDB ID: LmjF.36.6940), and *L. donovani* (TriTrypDB ID: LdBPK_367280.1) were included. The consensus sequence was then subjected to a BLAST analysis against the *L. braziliensis* genome (M2904 MHOM/BR/75 M2903) using the TriTrypDB server. The identified candidates were analysed by percentage identity, e-value, and functional domains using InterPro (Mitchell et al. 2019). The physical-chemical properties and signal peptide of the candidate protein LbPDI2 was predicted using ProtParam and SignalP 6.0, respectively (Wilkins et al. 1999; Teufel et al. 2022). Furthermore, a computational model of the candidate's tertiary structure was obtained using

AlphaFold 3 (Abramson et al. 2024) and validated using the Ramachandran plot with MolProbity (Davis et al. 2007). The visualization of the predicted structure was completed with ChimeraX (Meng et al. 2023). To explore conformational dynamics, the predicted LbPDI2 tertiary structure was subjected to simulations using the CABS-flex 3.0 server under default parameters. Local residue flexibility was assessed via root mean square fluctuation (RMSF) analysis to identify highly mobile regions throughout the simulation trajectory (Nithin et al., 2024).

2. Experimental approach

2.1. Cell culture

L. braziliensis promastigotes (MHOM/BR/75/M2903) (LbWT), LbCas9/T7, and the LbPDI2$^{-/-}$ knockout cell lines were cultured at 26°C in M199 medium (Sigma Aldrich M2520) supplemented with 2.2 g/L $NaHCO_3$, 0.005% (w/v) hemin, 40 mM L-glutamine, and 10% (v/v) fetal bovine serum (FBS) (Biowest S1810-500). Selection drugs were added to the medium at the following final concentrations: 35 µg/mL hygromycin B (HyClone SV30070.01) for the LbCas9/T7 strain and 20 µg/mL puromycin dihydrochloride (Santa Cruz Biotechnology sc108071B) as the selection drug to obtain the LbPDI2$^{-/-}$ strain. In addition, each culture was treated with 10 U/mL penicillin and 10 µg/mL streptomycin to prevent microbial contamination (León et al. 2025).

2.2. Synthesis of single guide RNA templates and repair DNA

The mutants used in this study were generated employing the kinetoplastid CRISPR/Cas9 toolkit (Beneke et al. 2017; Beneke and Gluenz 2019). The *Lbpdi2* gene ID LBRM2903_350086300.1 was used to retrieve from the LeishGEdit platform the required primers for the generation of sgRNA templates (5'sgRNA LbPDI2, 3'sgRNA LbPDI2 and Scaffold primer) and repair DNA (UpFwLbPDI2 and UpRvLbPDI2) through PCR amplification. Primer sequences are detailed in **Table S1**.

For amplification of repair DNA, 34 µL nuclease free water (H_2O), 10 µL buffer 5X (Accuris 5X High fidelity Reaction Buffer) supplemented with 5 mM dNTPs and 15 mM $MgCl_2$, 0,4 µM each of gene-specific forward and reverse primers (UpFwLbPDI2 and UpRvLbPDI2), 1 Unit HiFi Polymerase (Accuris High Fidelity Polymerase) and 1 µL of pTpuro plasmid (50 ng) were mixed in 50 µL total volume. PCR steps were 5 min at 94°C followed by 35 cycles of 30 s at 94°C, 30 s at 65°C, 2 min 15 s at 72°C followed by a final elongation step for 7 min at 72°C. One microliter of this reaction was run on a 1% (w/v) agarose gel to check for the presence of the expected product. The remainder was heat-sterilized at 94°C for 5 min and used for transfection without further purification. For electroporation, the reaction was set up in duplicate.

For amplification of sgRNA templates, 5 µL H_2O, 5 µL buffer 5X (Accuris 5X High fidelity Reaction Buffer) supplemented with 5 mM dNTPs and 15 mM $MgCl_2$, 0.2 µM of 5'sgRNA LbPDI2 or 3'sgRNA LbPDI2 and 5

μM of Scaffold primer, and 0.5 Unit HiFi Polymerase (Accuris High Fidelity Polymerase) were mixed in 20 μL total volume. PCR steps were 30 s at 98°C followed by 30 cycles of 10 s at 98°C, 30 s at 60°C, 15 s at 72°C. One microliter of these reactions was run on a 1% (w/v) agarose gel to check for the presence of the expected products. The remainder was heat-sterilized at 94°C for 5 min and transfected without further purification. For electroporation, the reaction was set up in duplicate.

2.3. Obtention of *L. braziliensis Lbpdi2*$^{-/-}$ promastigotes

L. braziliensis promastigotes expressing SpCas9 and T7RNAP (LbCas9/T7) were obtained from a previous study (León et al. 2023). Parasites in mid-log phase (10^8 cells/mL) were placed in electroporation buffer EPB (21 mM HEPES pH 7.5, 137 mM NaCl, 5 mM KCl, 0.7 mM Na_2HPO_4, 6 mM glucose) and mixed with pooled repair DNA, 5'sgRNA and 3'sgRNA (140 μL) in a pre-chilled 2 mm electroporation cuvette (BioRad). Electroporation was performed using a Bio-Rad Gene Pulser Xcell System (1 pulse, 400 V, infinite resistance, 500 μF) followed by subsequent selection in M199 medium supplemented with 20 μg/mL puromycin dihydrochloride in a 25 mL cell culture flask. Cultures were monitored for 4 weeks. This process resulted in the isolation of a resistant strain denoted *LbPDI2*$^{-/-}$.

2.4. Diagnostic PCRs

Genomic DNA was extracted 4 weeks post-transfection with gDNA extraction buffer (10 mM TRIS-HCl pH 8.5, 5 mM EDTA, 0.5% (w/v) SDS, 200 mM NaCl, 100 μg/mL proteinase K) from 5 mL of culture. One hundred nanograms of purified gDNA was mixed with 9.1 μL H_2O, 1.5 μL Buffer 10X, 1.5 μL $MgCl_2$ 25 mM, 0.3 μL dNTPs mix 10 μM, 0.3 μL forward and reverse diagnostic primers (10 μM each, sequences are detailed in **Table S1**) and 1 Unit Taq Polymerase in 15 μL total volume. PCR steps were 5 min at 94°C followed by 30 cycles of 30 s at 94°C, 30 s at 62°C, 30 s at 72°C followed by a final elongation step for 10 min at 72°C. Three microliters of this reaction were run on a 1% (w/v) agarose gel to check for the presence of the expected products.

2.5. Sanger sequencing

To sequence repair DNA at the integration sites, PCR amplicons obtained with Fw Diag PDI2 and Rv Diag PDI2 (**Table S1**), were run on a 1% (w/v) agarose gel TAE buffer, the band excised from the gel, and purified using the Squeeze and Freeze method (Thuring et al. 1975). Sanger sequencing of the amplicon was performed by Instituto de Genética, Universidad Nacional de Colombia (IGUN).

2.6. Growth curves

LbWT and LbPDI2$^{-/-}$ parasites in the mid-log phase (10^8 promastigotes/mL) were counted on a hemocytometer and prepared at a concentration of $5x10^5$ promastigotes/mL in M199 medium supplemented with 10% FBS in the absence of antibiotics. The parasites were seeded into a sterile 24-well culture plate, incubated at 26°C and counted in triplicate at 24h intervals until the stationary phase was reached after five days. Three biological replicates were performed.

2.7. Pharmacological susceptibility assays

The susceptibility of LbWT and LbPDI2$^{-/-}$ parasites to hydrogen peroxide, antimony potassium tartrate (Sb^{3+}), geneticin G418, and ketoconazole was assessed using an MTT assay. Briefly, 50 µL of promastigotes at 10x^{6} parasites/mL in the mid-log phase were cultured in a 96-well plate with 50 µL of different concentrations of the substances for 48 h at 27°C. After treatment, 10 µL of sterile MTT solution (5 mg/mL) was added and incubated at 37°C for 4h. The formazan crystals generated were dissolved by adding 100 µL of SDS 10% (w/v)-HCl 0.01M solution and absorbance readings were taken at 540 nm. Data from treated and untreated cultures were used to calculate the 50% effective concentration (EC_{50}) by sigmoidal regression analysis (normalized response with variable slope) using GraphPad Prism software (10.3.1). Untreated control parasites and reagent blanks were included in each technical replicate. The assays were performed in technical triplicate and at least two biological replicates (León et al. 2025).

2.8. Flow cytometry measurements

One mL of LbWT and LbPDI2$^{-/-}$ promastigotes in the exponential growth phase, cultured in M199 medium supplemented with 10% (v/v) FBS, were treated with H_2O_2 (6 mM) and G418 (EC_{50}) in 24-well plates for 48 hours. The parasites were centrifuged at 3000 rpm for 10 minutes and washed with cold PBS. The promastigotes were stained with 7-AAD and annexin V conjugated to phycoerythrin, following the manufacturer's instructions (Muse). The cells were then analyzed using the Muse Cell Analyzer flow cytometer to determine necrosis and apoptosis-like events, including 2000 events per sample.

3. RESULTS

3.1 A PDI2 candidate was identified in *L. braziliensis*.

To identify a PDI2 in *L. braziliensis*, a bioinformatic search was conducted using the consensus sequence of the open reading frames (ORFs) alignment of experimentally characterized PDI2 from New and Old-World species of the parasite, including *L. amazonensis*, *L. major*, and *L. donovani*. The bioinformatics search identified a candidate in the TriTrypDB database denoted as LbPDI2 (LBRM2903_350086300.1). Its inclusion into the multiple sequence alignment revealed extensive sequence conservation and the presence of two characteristic active sites (48-CGHC-51 and 382-CGHC-385) (Fig. 1A). Subsequent structural analysis revealed the presence of four functional domains (A, B, B', and A'), a predicted signal peptide (1-SP-20), and an intrinsically disordered region (462-IDR-470). Furthermore, a linker X region was identified between domains B' and A', and the occurrence of the EGDL sequence (467–470), which is necessary for protein retention in the ER, was observed (Laurindo et al., 2012; Zeke et al. 2024) (Fig. 1B). The bioinformatics search also identified five additional proteins, whose functional domains and active sites allow them to be included in the family of proteins related to disulfide isomerase activity. These include PDI6, PDI-A', the transmembrane PDI8, Erp29 (ER-resident protein 29), and thioredoxin (Table 1).

Table 1
Bioinformatically identified PDIs in *L. braziliensis*.

TriTrypDB code	Protein ID[1]	Identity (%)[2]	e-value	Residues	Redox-active site
LBRM2903_350086300.1	PDI2	78	0.0	470	CGHC / CGHC
LBRM2903_200027600.1	PDI6	34	$2e^{-18}$	433	CGHC
LBRM2903_060017300.1	PDI-A'	45	$9e^{-16}$	133	CGHC
LBRM2903_340018900.1	PDI8	35	$1e^{-08}$	563	CSHC
LBRM2903_260011500.1	Erp29	24	$8e^{-06}$	379	-
LBRM2903_010007600.1	Thioredoxin	32	$4e^{-04}$	107	CGPC

[1] According to the "Protein Features and Properties" option in TriTrypDB.

[2] Compared to the query consensus sequence.

Among the proteins identified by the bioinformatic search, the LbPDI2 candidate is the only one in the M2903 reference assembly that possesses the four functional domains and two CXXC active sites characteristic of this type of protein. Consequently, the *in silico* analysis at the tertiary structure level of the LbPDI2 candidate was continued by constructing a predictive model without the SP (1-MKLLYVVFFVCTLLLCLTSA-20) using AlphaFold 3. The structure demonstrated high confidence values (> 70%) in accordance with the predicted Local Distance Difference Test (pLDDT). However, the IDR (462–470) exhibited low confidence values (< 50%) due to its inherent propensity towards disorder. The predicted structure is consistent with a compact, U-shaped arrangement in which the catalytic domains A and A' oppose each other, separated by the structural domains B and B' (Fig. 2A). Furthermore, the structural quality of the LbPDI2 model was evaluated using the Ramachandran plot, which indicated a Rama-Z value of -0.06 (confident values < 2.0), 99.48% of residues in allowed regions, 97.77% of residues in favored regions, and N449 as the only outlier residue (Fig. 2B). This structural inference is based on *in silico* modelling, whose experimental validation by structural experiments is pending. Nonetheless, for *in silico* validation, the predicted LbPDI2 model was compared with X-ray crystallography-resolved tertiary structures. Specifically, the model was structurally superimposed onto the *Saccharomyces cerevisiae* PDI (PDB 2B5E). This analysis showed consistent overlap across all functional domains, except for the IDR, as expected for such challenging-to-resolve sequences. Consequently, the overall topology of LbPDI2 aligns with a canonical PDI, providing robust structural inferences for this candidate (Fig. 2C). Moreover, elevated root mean square fluctuation (RMSF) values, which indicate the relative propensities of protein residues to deviate from a mean dynamic structure, were observed in domain B and the IDR sequence, suggesting a high degree of conformational flexibility. These regions are potentially essential for the

open-to-closed state transition required for substrate structural adaptation of the LbPDI2 candidate (Fig. 2D).

The ORF of *Lbpdi2* is 1413 nucleotides in length. A comparison of the mRNA and genomic DNA revealed that the identified sequence lacks introns. Furthermore, this sequence is present as a single copy within the M2903 reference genome, as indicated by the synteny analysis displayed for this gene in the TriTrypDB, which supports the uniqueness of the candidate. Overall, sequence and structural analyses indicate that the identified ORF is evolutionarily conserved within the genus *Leishmania* and corresponds to a high-confidence functional PDI2 enzyme. Overall, sequence and structural analyses indicate that the identified ORF is evolutionarily conserved within the genus *Leishmania* and corresponds to a high-confidence functional PDI2 enzyme. Furthermore, since it shares the characteristic structural features of experimentally characterized orthologs, it can be formally classified as the functional LbPDI2 enzyme.

3.2 The deletion of LbPDI2 impacts the pharmacological susceptibility of promastigotes.

To investigate the role of LbPDI2 in diverse pharmacological treatments of *L. braziliensis* promastigotes, a CRISPR/Cas9-mediated deletion strategy was employed to generate the *Lbpdi2*$^{-/-}$ mutant parasite line. Initially, repair DNA (1914 bp) and sgRNA templates (124 bp) targeting the 5' and 3' ends of the gene of interest (GOI) were obtained, which are inputs required for the editing strategy that allows the GOI to be cut at both ends and replaced with repair DNA (Fig. 3A). Then, using *L. braziliensis* promastigotes transfected with the pTB007 Viannia plasmid, which allows overexpression of the SpCas9 endonuclease and the T7RNAP enzyme (LbCas9/T7 cell line), the sgRNA templates and repair DNA were electroporated to replace the LbPDI2 coding sequence with the puromycin resistance marker (rPuro: puromycin N-acetyltransferase). The successful replacement of the GOI was confirmed by diagnostic PCR using Fw and Rv primers that anneal to the 5' and 3' UTR regions, respectively. The expected amplicon size in the wild type (WT) is 2161 bp, while substitution by the rPuro marker generate a 2464 bp fragment in the LbPDI2$^{-/-}$ parasites (Fig. 3B). The implementation of an allele-discrimination PCR, using primers to the 5'UTR and an internal region of the *Lbpdi*2 ORF, indicates an expected product only in the WT and the Cas9/T7 isogenic background. However, the same product was not detected in the LbPDI2$^{-/-}$ mutant parasites (Fig. 3C). This result confirms that the gene of interest was deleted after selection and supports the observation that there are no extra copies of the LbPDI2 gene in the M2903 reference genome, as suggested by the synteny analysis from TriTrypDB. Sanger sequencing of the 2464 bp product confirmed the obtention of the LbPDI2$^{-/-}$ mutant parasite line and demonstrated on-target integration of the repair DNA at the LbPDI2 locus (Fig. 3D). The absence of LbPDI2 in the protein extracts of the mutant parasites was confirmed by LC-MS/MS analysis (data not shown). Even though this strategy resulted in the generation of a puromycin-resistant population that was designated as LbPDI2$^{-/-}$, clonal isolation and independent knockout lines were not produced in this study, which may allow residual heterogeneity. Nevertheless, the LbPDI2$^{-/-}$ mutant population constitutes a preliminary step to conduct phenotypic assays focused on drug stress-response of the promastigotes.

The effect of the deletion on the growth of promastigotes at 26°C in M199 medium supplemented with FBS and without selection antibiotics was determined. Growth curves for both WT and LbPDI2$^{-/-}$ cell lines exhibited comparable patterns indicating that LbPDI2 is not essential for basal proliferation (Fig. 4A). Subsequently, the pharmacological susceptibility of promastigotes to substances that exert different mechanisms of action, some of which are used clinically, was determined by implementing cell viability assays based on the MTT method and EC_{50} determination. Promastigote susceptibility assays were used as a preliminary screen to assess stress-response phenotypes prior to evaluation in intracellular amastigotes.

Susceptibility assays were conducted in the absence of selection antibiotics to minimize the effects of acute drug exposure. Additionally, comparisons were made to WT rather than to a Cas9/T7 puromycin-matched isogenic control, as this work represents an initial screen using a validated CRISPR/Cas9 platform. The objective of this approach was to avoid the effects associated with Cas9/T7 expression, unspecific integration events and prior drug selection, which have the potential to alter metabolism in that control.

The analysis began by evaluating the susceptibility of parasites to H_2O_2, a molecule that generates reactive oxygen species (ROS), since macrophages combat microorganisms through oxidative bursts and acidification of parasitophore vesicles (Kawakami et al., 2016). The results showed that the response of LbPDI2$^{-/-}$ parasites exhibited a slight but not significant increase in EC_{50} compared to WT parasites (268.8 ± 29.5 µM *vs* 227.5 ± 2.2 µM). This suggests that LbPDI2 does not play a direct role in the antioxidant response of *L. braziliensis* to H_2O_2 (Fig. 4B and Table 2).

Then, considering that PDI2 exerts oxidoreductase, isomerase, and chaperone activity on proteins containing cysteine residues, the effect of exposure to thiophilic substances such as Sb^{3+} – the active component in first-line antimony-based drugs that is effective against promastigotes – was evaluated. It was observed that EC_{50} values increased for Sb^{3+} in LbPDI2$^{-/-}$ parasites compared to WT (1.23 ± 0.07 µg/mL *vs* 0.64 ± 0.17 µg/mL) (Fig. 4B and Table 2).

Subsequently, the response to substances that affect protein synthesis was evaluated. These substances include the broad-spectrum aminoglycoside ribosome inhibitor geneticin G418, which is used against eukaryotic pathogens. The EC_{50} value of LbPDI2$^{-/-}$ parasites in response to G418 is reduced compared to WT (2.24 ± 1.6 µg/mL *vs* 9.5 ± 1.2 µg/mL), suggesting that LbPDI2 plays an important role in the parasite's defence against molecules that affect protein synthesis (Fig. 4B and Table 2).

Furthermore, the effect of ketoconazole, a prominent inhibitor of sterol 14α-demethylase (CYP51) protein, a key enzyme situated in the glycosome (Jamdhade et al. 2015) and in the ER of the parasite, was evaluated. This enzyme participates in the synthesis of ergosterol, a significant component of the parasite's cell membranes (Verma et al. 2011). Inhibition of CYP51 causes accumulation of 14-methylated sterols, inducing ER stress due to lipid homeostasis imbalance (Zhang et al. 2016; Binjubair

et al. 2020). In this study, a decrease in the EC_{50} for ketoconazole was observed in LbPDI2$^{-/-}$ parasites compared to WT (4.61 ± 1.2 µg/mL *vs* 19.0 ± 3.3 µg/mL), suggesting that LbPDI2 participates in the response to attenuate ER stress generated by lipid accumulation (Fig. 4B and Table 2).

Table 2
Pharmacological susceptibility profile.

Substance	**EC_{50}[1]**		**Relative resistance[2]**
	LbWT	**LbPDI2$^{-/-}$**	
H_2O_2 (µM)	227.5 ± 2.2	268.8 ± 29.5	1.18
Sb^{3+} (µg/mL)	0.64 ± 0.17	1.23 ± 0.07	1.92
G418 (µg/mL)	9.5 ± 1.2	2.24 ± 1.6	0.23
Ketoconazole (µg/mL)	19.0 ± 3.3	4.61 ± 1.2	0.24

[1] EC_{50} values correspond to the mean ± S.D. of two independent experiments performed in technical triplicate.

[2] The relative resistance corresponds to EC_{50} LbPDI2$^{-/-}$ / EC_{50} LbWT.

EC_{50} trends were consistent across technical and biological replicates conducted with the LbPDI2$^{-/-}$ mutant population without clonal derivatives or genetic complementation assays. Therefore, the results of the pending add-back experiments and the analysis of independent clones will strengthen the observation that the LbPDI2 deletion alters the parasite's response to pharmacological stress.

Given LbPDI2's role as an ER-associated oxidoreductase, it is important to note that redox-dependent colorimetric readouts, such as MTT, may be particularly sensitive to changes in metabolic state. It would therefore be advisable to corroborate the EC_{50} estimates by conducting additional viability assays, such as resazurin, ATP-luminescence or live/dead flow cytometry. In this regard, preliminary flow cytometry measurements were carried out to rule out any redox-dependent artefacts in the MTT assay. These measurements, based on annexin V and 7-AAD staining, demonstrated survival differences among the control and H_2O_2 and G418 treatments in the LbWT and LbPDI2$^{-/-}$ mutant population, using a non-redox viability measure (Fig. 4C). These findings indicate parasite death, potentially via apoptosis-like, confirming that MTT assay results are not attributable to redox-dependent artefacts.

4. DISCUSSION

Leishmaniasis remains a NTD that predominantly affects populations in tropical regions with limited access to healthcare. The absence of an effective vaccine, the limitations of current treatments, and the emergence of drug resistance highlight the urgent need to identify novel therapeutic targets through

biochemical and molecular studies of the parasite. In this context, the present study reports the identification and structural analysis of a candidate gene encoding protein disulfide isomerase 2 in *L. braziliensis* (LbPDI2) and evaluates the effects of its deletion by CRISPR/Cas9 in promastigotes.

PDIs are a family of enzymes that catalyze the formation, reduction, and isomerization of disulfide bonds, playing a crucial role in protein folding within the ER. This function is essential for maintaining cellular proteostasis and preventing toxicity associated with ER stress. Structurally, PDI2 is characterized by two thioredoxin-like catalytic domains (A and A'), separated by non-catalytic domains (B and B'), a flexible linker region, and a C-terminal ER retention signal. The catalytic domains contain the conserved CXXC motif, whose cysteine residues are directly involved in the enzyme's oxidoreductase and isomerase activities (Kushawaha et al. 2012).

Using bioinformatic approaches, six PDI candidates were identified in *L. braziliensis*. However, only the candidate designated as LBRM2903_350086300.1 in the TriTrypDB database exhibited the full set of canonical structural features of PDI2, including domains A, A', B, and B', as well as the characteristic CGHC catalytic motifs. Additionally, the presence of an N-terminal signal peptide, an intrinsically disordered region, and an ER retention sequence (EGDL) supports its role in ER-associated proteostasis. Nevertheless, given that PDI2 has been detected in the secretome of other *Leishmania* species (Cuervo et al. 2009; Pissarra et al. 2022), further studies are required to determine its localization and functional relevance during infection in *L. braziliensis*.

Structural modeling of LbPDI2 revealed a typical U-shaped conformation, with an internal hydrophobic pocket formed by domains B and B'. This configuration facilitates the binding of unfolded or partially folded polypeptides, particularly those exposing hydrophobic regions (Tian et al. 2006). The linker region provides conformational flexibility, allowing the protein to transition between open and closed states and enabling the catalytic domains to adjust to substrates of varying sizes (Wang et al. 2012). Additionally, the elevated flexibility within domain B and the IDR sequence facilitates the conformational transitions of LbPDI2, as indicated by its RMSF profile.

Although PDIs have been studied in several *Leishmania* species, including *L. major* (Achour et al. 2002), *L. donovani* (Kushawaha et al. 2012), *L. amazonensis* (Hong and Soong 2008), and *L. tropica* (Ali et al. 2016), PDI2 had not been specifically characterized in *L. braziliensis*. To address this gap, this study employed CRISPR/Cas9-mediated gene editing to obtain LbPDI2 knockout promastigotes and investigate the functional consequences of its deletion.

The deletion of *Lbpdi2* was not lethal, suggesting the presence of compensatory mechanisms mediated by other PDIs, such as Erp29, PDI-A', PDI6, and PDI8 (Table 1). Similar compensatory responses have been described in other organisms, where the loss of one PDI is offset by the upregulation of others. For instance, to obtain the PDI1$^{-/-}$ mutant, which is lethal in *Saccharomyces cerevisiae*, it is necessary to induce the overexpression of its other four PDIs (Nøgaard et al. 2003). In the case of *Haemaphysalis longicornis*, a decrease in PDI2 expression leads to an increase in HlPDI1 and HlPDI3 expression as a

compensatory mechanism (Liao et al. 2008). Future studies comparing expression levels of PDI family members in LbWT and LbPDI2$^{-/-}$ mutant parasites would help validate this hypothesis.

To assess the functional impact of LbPDI2 deletion, susceptibility assays were conducted using agents that induce oxidative stress, disrupt lipid biosynthesis, or interfere with protein translation. No significant differences were observed among LbWT and LbPDI2$^{-/-}$ mutant parasites upon treatment with H_2O_2, consistent with previous findings indicating that oxidative stress does not substantially alter PDI expression in other study models (Pierre et al. 2014).

In contrast, LbPDI2$^{-/-}$ promastigotes exhibited increased susceptibility to ketoconazole and the aminoglycoside G418. Ketoconazole inhibits ergosterol biosynthesis, leading to the accumulation of abnormal sterols, disruption of lipid homeostasis, and ER stress (Vannier-Santos et al. 1995; Zhang et al. 2016). In the absence of LbPDI2, these effects are exacerbated due to impaired protein folding capacity, resulting in enhanced cellular stress.

Similarly, G418 interferes with protein synthesis by inducing translational errors and generating unfolded proteins. While cells typically respond by upregulating oxidoreductases and other protective mechanisms (Hoppe et al. 2003; Shalev et al. 2013), the lack of LbPDI2 compromises the ability to refold or eliminate unfolded proteins. Consequently, LbPDI2$^{-/-}$ mutant parasites experience increased ER stress and reduced viability, as observed here.

The deletion of LbPDI2 did not yield a generalized hypersensitivity to all tested stressors, as would be anticipated from the disruption of a proteostasis core component. Conversely, the mutant parasites exhibited increased resistance to Sb^{3+}, while displaying heightened sensitivity to G418 and ketoconazole. This differential phenotype indicates that LbPDI2 exerts a specialized role in the orchestration of specific cellular stress responses rather than a broad, non-specific function. These data indicate that LbPDI2 functions beyond a canonical chaperone, specifically mediating the parasite's phenotypic plasticity against distinct pharmacological stressors. Consequently, our findings suggest that the disruption of LbPDI2-mediated proteostasis represents a strategic molecular target for the development of synergistic combination therapies.

As the LbPDI2$^{-/-}$ line was generated in an LbCas9/T7 background and selected with puromycin, it is not possible to exclude background effects from nuclease expression or cassette integration in the phenotypic assays (Fig. 4). Future work will incorporate isogenic LbCas9/T7, puromycin-matched controls, as well as add-back lines to rigorously isolate LbPDI2-specific effects. Furthermore, given that all functional data were generated in promastigotes with Sb^{3+}, translatability to intracellular amastigotes and to clinically used pentavalent antimonials (Sb^{5+}) remains to be established.

In conclusion, this study identifies LbPDI2 as a protein that exhibits the canonical structural features of experimentally characterized PDI2 orthologs, and demonstrates its role in modulating drug susceptibility in *L. braziliensis* promastigotes. The heightened sensitivity of LbPDI2-deficient parasites to specific

pharmacological agents underscores the protein's critical importance for parasite survival under stress. These findings elucidate the contribution of LbPDI2 to the promastigote stress response, while further investigations in intracellular amastigotes and with Sb^{5+} are necessary to establish its full therapeutic relevance. Ultimately, this work justifies the exploration of LbPDI2 as a promising target for the development of improved anti-leishmanial strategies.

Declarations

ACKNOWLEDGEMENTS

This work was funded by Universidad Nacional de Colombia, grants 57423 (MHR), 63428 and 62175 (LECR). Pre-submission review was conducted using *qed Science* (https://www.qedscience.com).

AUTHORSHIP CONTRIBUTION STATEMENT

PEM Villanueva: conceptualization, investigation, methodology, formal analysis, writing-original draft.

Esteban León: investigation, methodology, formal analysis.

Adrián G Sandoval-Hernández: investigation, methodology, formal analysis.

Maria H Ramírez-Hernández: conceptualization, methodology, formal analysis, resources.

Luis E Contreras R:conceptualization, methodology, formal analysis, supervision, resources, project administration, writing-review and editing.

FUNDING SOURCES

This work was funded by Universidad Nacional de Colombia, grants 57423 (MHR), 63428 and 62175 (LECR).

DECLARATION OF COMPETING INTERESTS

The authors have no relevant financial or non-financial interests to disclose.

References

1. Abramson J, Adler J, Dunger J et al (2024) Accurate structure prediction of biomolecular interactions with AlphaFold 3. Nature 630. https://doi.org/10.1038/s41586-024-07487-w
2. Achour Y, Ben, Chenik M, Louzir H, Dellagi K (2002) Identification of a disulfide isomerase protein of Leishmania major as a putative virulence factor. Infect Immun 70. https://doi.org/10.1128/IAI.70.7.3576-3585.2002
3. Ali D, Abbady AQ, Kweider M, Soukkarieh C (2016) Cloning, expression, purification and characterization of Leishmania tropica PDI-2 protein. Open Life Sci 11. https://doi.org/10.1515/biol-

2016-0022

4. Alpizar-Sosa EA, Ithnin NRB, Wei W et al (2022) Amphotericin B resistance in Leishmania mexicana: Alterations to sterol metabolism and oxidative stress response. PLoS Negl Trop Dis 16. https://doi.org/10.1371/journal.pntd.0010779
5. Beneke T, Gluenz E (2019) LeishGEdit: A Method for Rapid Gene Knockout and Tagging Using CRISPR-Cas9. Methods in Molecular Biology. Humana Press Inc., pp 189–210
6. Beneke T, Madden R, Makin L et al (2017) A CRISPR Cas9 high-throughput genome editing toolkit for kinetoplastids. R Soc Open Sci 4:1–16. https://doi.org/10.1098/rsos.170095
7. Binjubair FA, Parker JE, Warrilow AG et al (2020) Small-Molecule Inhibitors Targeting Sterol 14α-Demethylase (CYP51): Synthesis, Molecular Modelling and Evaluation Against Candida albicans. https://doi.org/10.1002/cmdc.202000250. ChemMedChem 15:
8. Cuervo P, De Jesus JB, Saboia-Vahia L et al (2009) Proteomic characterization of the released/secreted proteins of Leishmania (Viannia) braziliensis promastigotes. J Proteom 73. https://doi.org/10.1016/j.jprot.2009.08.006
9. Davis IW, Leaver-Fay A, Chen VB et al (2007) MolProbity: All-atom contacts and structure validation for proteins and nucleic acids. Nucleic Acids Res 35. https://doi.org/10.1093/nar/gkm216
10. Dinc R (2022) Leishmania Vaccines: the Current Situation with Its Promising Aspect for the Future. Korean J Parasitol 60
11. Dousti M, Hosseinpour M, Ghasemi ND et al (2023) The potential role of protein disulfide isomerases (PDIs) during parasitic infections: a focus on Leishmania spp. Pathog Dis 81
12. Gutierrez Guarnizo SA, Tikhonova EB, Karamyshev AL et al (2023) Translational reprogramming as a driver of antimony-drug resistance in Leishmania. Nat Commun 14. https://doi.org/10.1038/s41467-023-38221-1
13. Hong BX, Soong L (2008) Identification and enzymatic activities of four protein disulfide isomerase (PDI) isoforms of Leishmania amazonensis. Parasitol Res 102. https://doi.org/10.1007/s00436-007-0784-4
14. Hoppe G, Chai YC, Sears J (2003) Endogenous oxidoreductase expression is induced by aminoglycosides. Arch Biochem Biophys. https://doi.org/10.1016/S0003-9861(03)00144-9. 414:
15. Jamdhade MD, Pawar H, Chavan S et al (2015) Comprehensive Proteomics Analysis of Glycosomes from Leishmania donovani. https://doi.org/10.1089/omi.2014.0163. OMICS 19:
16. Kushawaha PK, Gupta R, Tripathi CDP et al (2012) Evaluation of leishmania donovani protein disulfide isomerase as a potential immunogenic protein/vaccine candidate against visceral leishmaniasis. PLoS ONE 7. https://doi.org/10.1371/journal.pone.0035670
17. León E, Maya-Hoyos M, Ramírez-Hernández MH et al (2025) Upregulation of nicotinamide/nicotinate mononucleotide adenylyl transferase increases resistance to oxidative stress and antimony in promastigotes of Leishmania braziliensis. https://doi.org/10.1016/j.exppara.2025.108979. Exp Parasitol 275:

18. León E, Ortiz V, Pérez A et al (2023) Anti-SpCas9 IgY Polyclonal Antibodies Production for CRISPR Research Use. ACS Omega 8. https://doi.org/10.1021/acsomega.3c04273
19. Liao M, Boldbaatar D, Gong H et al (2008) Functional analysis of protein disulfide isomerases in blood feeding, viability and oocyte development in Haemaphysalis longicornis ticks. Insect Biochem Mol Biol 38. https://doi.org/10.1016/j.ibmb.2007.11.006
20. Mann S, Frasca K, Scherrer S et al (2021) A Review of Leishmaniasis: Current Knowledge and Future Directions. Curr Trop Med Rep 8
21. Matsusaki M, Kanemura S, Kinoshita M et al (2020) The Protein Disulfide Isomerase Family: from proteostasis to pathogenesis. Biochim Biophys Acta Gen Subj 1864. https://doi.org/10.1016/j.bbagen.2019.04.003
22. Meng EC, Goddard TD, Pettersen EF et al (2023) UCSF ChimeraX: Tools for structure building and analysis. Protein Sci 32. https://doi.org/10.1002/pro.4792
23. Mitchell AL, Attwood TK, Babbitt PC et al (2019) InterPro in 2019: Improving coverage, classification and access to protein sequence annotations. Nucleic Acids Res 47. https://doi.org/10.1093/nar/gky1100
24. Nithin C, Fornari RP, Pilla SP et al (2024) Exploring protein functions from structural flexibility using CABS-flex modeling. Protein Sci 33. https://doi.org/10.1002/pro.5090
25. Nøgaard P, Tachibana C, Bruun AW, Winther JR (2003) Gene regulation in response to protein disulphide isomerase deficiency. Yeast 20. https://doi.org/10.1002/yea.978
26. Notredame C, Higgins DG, Heringa J (2000) T-coffee: A novel method for fast and accurate multiple sequence alignment. J Mol Biol 302. https://doi.org/10.1006/jmbi.2000.4042
27. Peláez RG, Muskus CE, Cuervo P, Marín-Villa M (2012) Expresión diferencial de proteínas en leishmania (Viannia) panamensis asociadas con mecanismos de resistencia a antimoniato de meglumina. Biomedica 32. https://doi.org/10.7705/biomedica.v32i3.392
28. Pierre N, Barbé C, Gilson H et al (2014) Activation of ER stress by hydrogen peroxide in C2C12 myotubes. Biochem Biophys Res Commun 450. https://doi.org/10.1016/j.bbrc.2014.05.143
29. Pissarra J, Pagniez J, Petitdidier E et al (2022) Proteomic Analysis of the Promastigote Secretome of Seven Leishmania Species. J Proteome Res 21. https://doi.org/10.1021/acs.jproteome.1c00244
30. Shalev M, Kondo J, Kopelyanskiy D et al (2013) Identification of the molecular attributes required for aminoglycoside activity against Leishmania. Proc Natl Acad Sci U S A 110. https://doi.org/10.1073/pnas.1307365110
31. Tasbihi M, Shekari F, Hajjaran H et al (2020) Comparative mitochondrial proteomics of Leishmania tropica clinical isolates resistant and sensitive to meglumine antimoniate. Parasitol Res 119. https://doi.org/10.1007/s00436-020-06671-x
32. Teufel F, Almagro Armenteros JJ, Johansen AR et al (2022) SignalP 6.0 predicts all five types of signal peptides using protein language models. Nat Biotechnol 40. https://doi.org/10.1038/s41587-021-01156-3

33. Thuring RWJ, Sanders JPM, Borst P (1975) A freeze-squeeze method for recovering long DNA from agarose gels. Anal Biochem 66. https://doi.org/10.1016/0003-2697(75)90739-3
34. Tian G, Xiang S, Noiva R et al (2006) The crystal structure of yeast protein disulfide isomerase suggests cooperativity between its active sites. Cell 124. https://doi.org/10.1016/j.cell.2005.10.044
35. Vannier-Santos MA, Urbina JA, Martiny A et al (1995) Alterations Induced by the Antifungal Compounds Ketoconazole and Terbinafine in Leishmania. J Eukaryot Microbiol. https://doi.org/10.1111/j.1550-7408.1995.tb01591.x. 42:
36. Verma S, Mehta A, Shaha C (2011) CYP5122A1, a novel cytochrome P450 is essential for survival of Leishmania donovani. PLoS ONE 6. https://doi.org/10.1371/journal.pone.0025273
37. Wang C, Yu J, Huo L et al (2012) Human protein-disulfide isomerase is a redox-regulated chaperone activated by oxidation of domain a'. J Biol Chem 287. https://doi.org/10.1074/jbc.M111.303149
38. Waterhouse AM, Procter JB, Martin DMA et al (2009) Jalview Version 2-A multiple sequence alignment editor and analysis workbench. Bioinformatics 25. https://doi.org/10.1093/bioinformatics/btp033
39. Wilkins MR, Gasteiger E, Bairoch A et al (1999) Protein identification and analysis tools in the ExPASy server. Methods Mol Biol 112
40. Zhang M, Yu Q, Liang C et al (2016) Lipid homeostasis is involved in plasma membrane and endoplasmic reticulum stress in Pichia pastoris. Biochem Biophys Res Commun 478. https://doi.org/10.1016/j.bbrc.2016.08.024

Figures

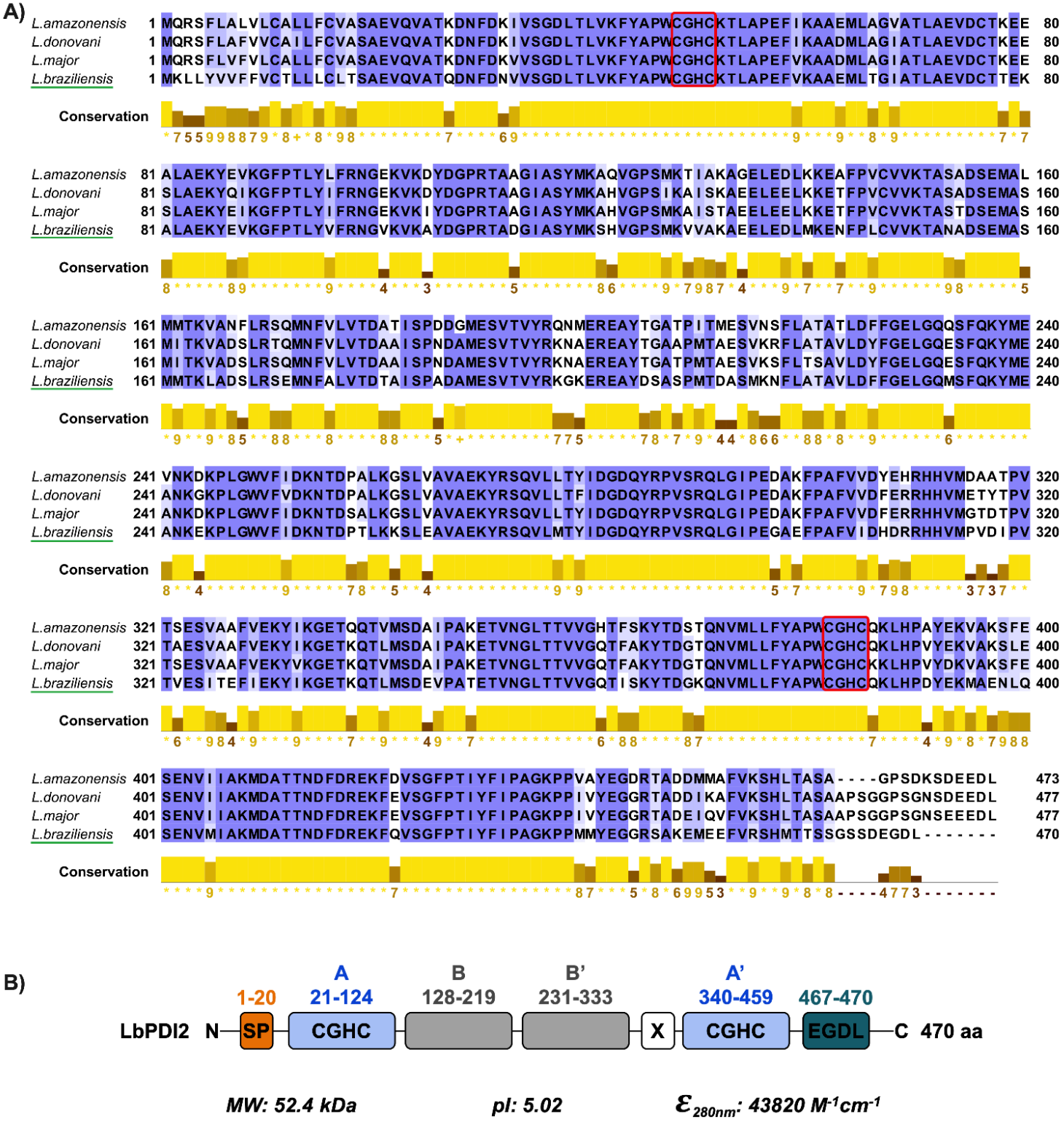


Figure 1

The LbPDI2 candidate exhibits canonical characteristics at the primary structure level. A) Multiple sequence alignment of *Leishmania* PDI2 ORFs showed highly conserved residues, which are highlighted in purple, according to the BLOSUM62 scoring system. The height of the yellow bars indicates the degree of conservation among the sequences. The predicted active sites are shown by red squares. The LbPDI2 candidate is underlined in green. The multiple sequence alignment was generated with Jalview 2.11.5.1.

B) The primary structural elements of the LbPDI2 candidate include a predicted signal peptide (SP), four functional domains (A, A', B, and B'), a linker X region, and an EGDL sequence necessary for retention at the ER. Predicted physical-chemical properties are included.

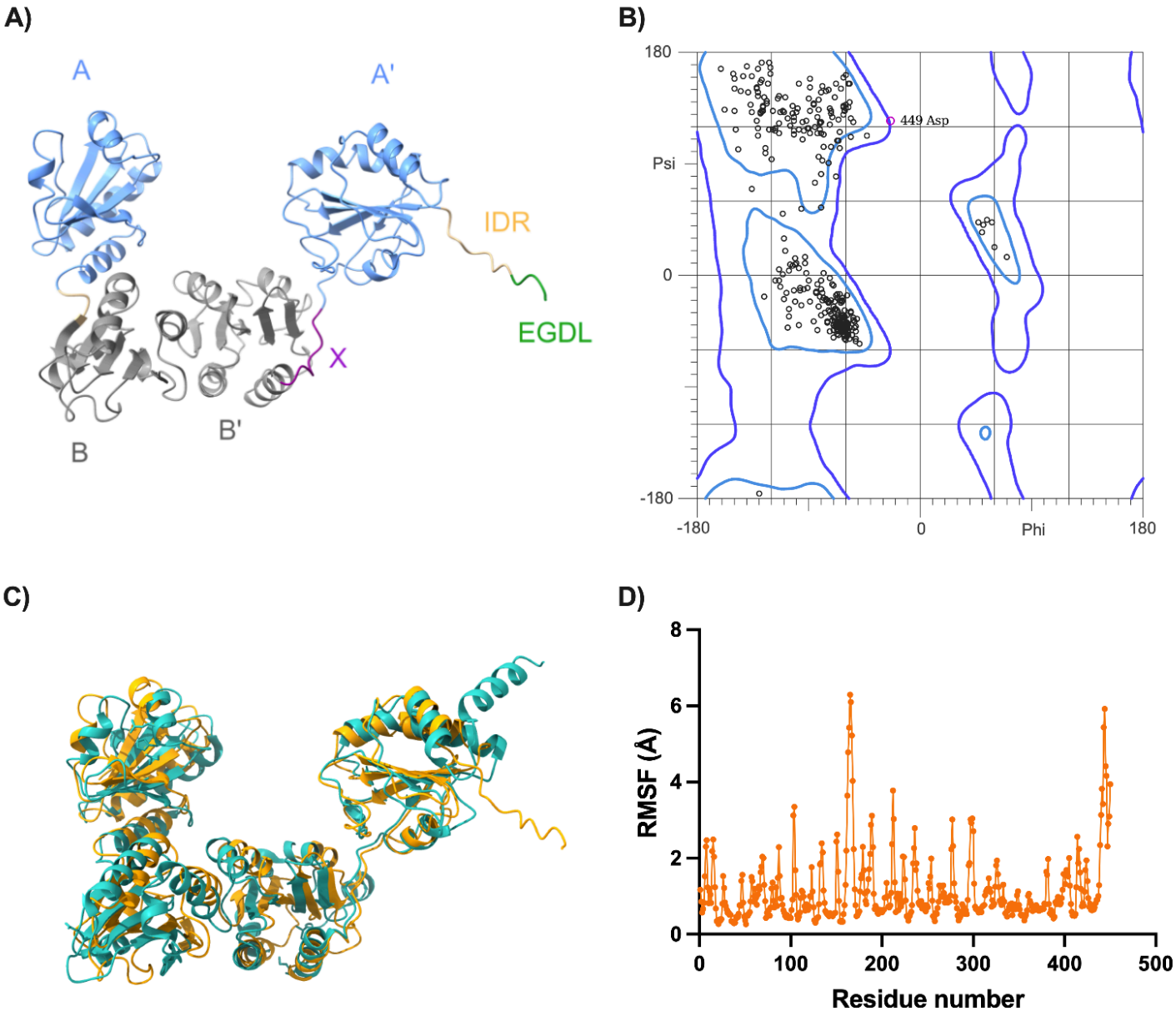


Figure 2

Tertiary structure model of the LbPDI2 candidate. A) The predicted tertiary structure of the LbPDI2 candidate was generated using AlphaFold3. The model was built for residues 21–470 due to the SP being excluded from the full sequence. IDR: intrinsically disordered region. Image generated with ChimeraX. **B)**Ramachandran plot showing the *phi (φ)* and *psi (ψ)* angles of the LbPDI2 candidate. Plot generated with MolProbity. **C)** Structural superposition of the tertiary structures of the LbPDI2 model (yellow) and the resolved PDI from *S. cerevisiae* (PDB 2B5E) (green), using Matchmaker. Image generated with ChimeraX. **D)** Structural flexibility analysis of LbPDI2. RMSF plot generated with CABS-

flex 3.0, showing elevated atomic fluctuations of residues located at domain B and the IDR sequence. Peaks indicate regions with high conformational mobility.

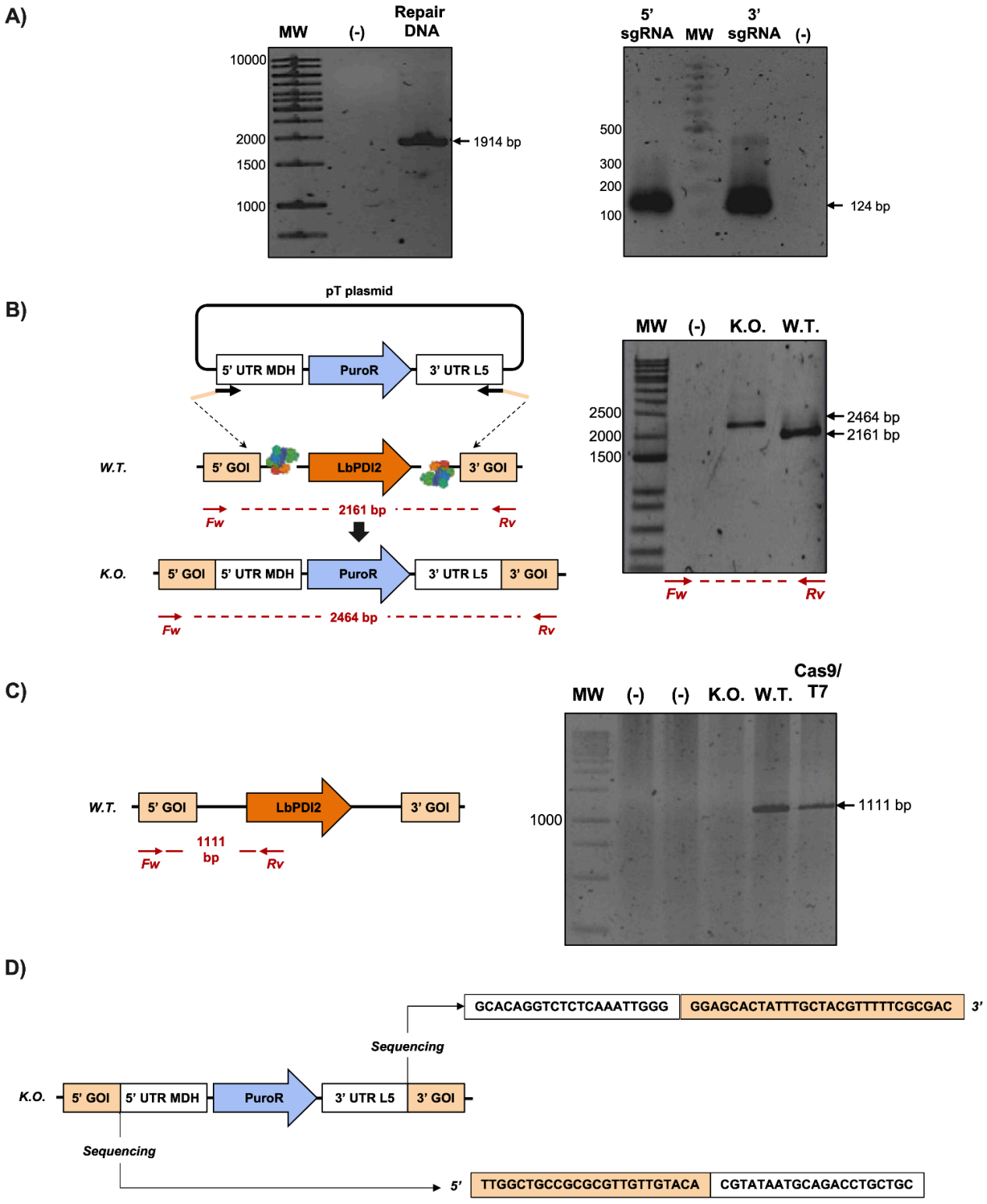


Figure 3

Editing of the *Lbpdi2* candidate gene was corroborated at the expected site. A) PCR amplification of repair DNA from the pT-Puro plasmid to replace the *Lbpdi2*GOI (left gel), and sgRNA templates directed

against the 5' and 3' regions of the *Lbpdi2* GOI (right gel). 1% and 2% (w/v) agarose gels in TBE, respectively. Ethidium bromide staining. MW, molecular weight (bp). **B)** Editing strategy for knocking out the *Lbpdi2* GOI. The diagnostic primers that generate different amplification sizes in the CRISPR-edited parasites (K.O.) are indicated in red. 1% (w/v) agarose gel in TBE. Ethidium bromide staining. MW: molecular weight (bp). **C)** Confirmation of the deletion of the *Lbpdi2*GOI by allele-discrimination PCR using the indicated primers. 1% (w/v) agarose gel in TBE. Ethidium bromide staining. MW: molecular weight (bp). **D)** The edited parasite line was confirmed by DNA sequencing at the 5' and 3' UTRs. The obtained sequences are shown.

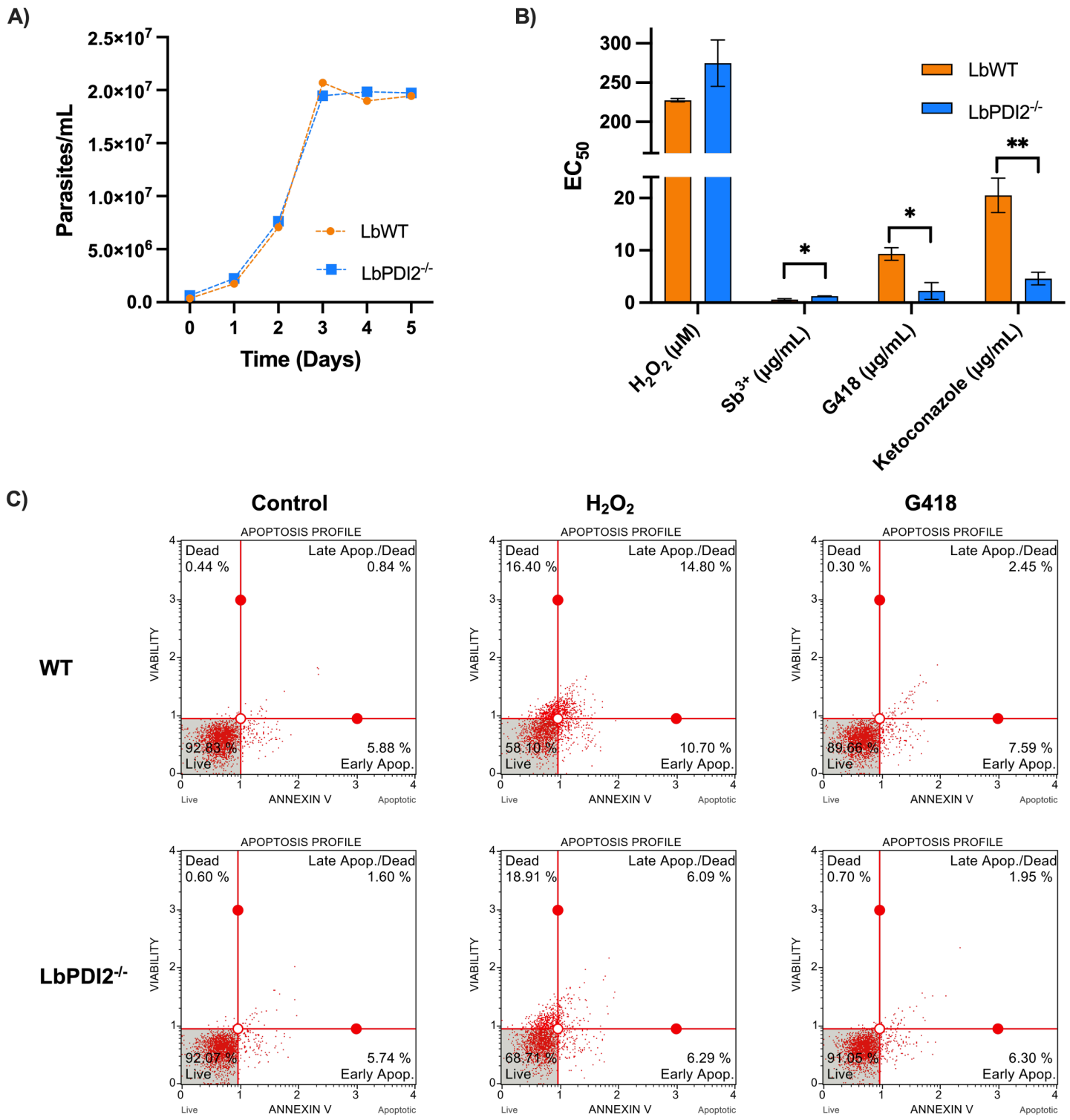


Figure 4

Phenotypic analysis of the LbPDI2$^{-/-}$ promastigotes. A) Growth kinetics of LbWT and LbPDI2$^{-/-}$ parasites. **B)** Drug susceptibility profile of LbWT and LbPDI2$^{-/-}$ parasites. EC_{50} values correspond to the mean ± S.D. of two independent experiments performed in technical triplicate. Values were calculated using GraphPad Prism (10.3.1). Asterisks indicate significant differences as determined by one-way ANOVA followed by Tukey's multiple comparisons test, *P < 0.05; **P < 0.01. **C)** Dot plots showing cell death in

LbWT and LbPDI2$^{-/-}$ promastigotes in the absence of drugs or following treatment with H_2O_2 (6 mM) or G418 (EC_{50}). The data are based on the analysis of 2,000 events per sample.

Supplementary Files

This is a list of supplementary files associated with this preprint. Click to download.

- Supplementarymaterial.docx